COPY / SCAN Received: December 23, 2005

Washington University Interlibrary Loan

ILLiad TN: 220073

Call # : **QC176 T45**

Location: **Phys General Stacks**

Journal Title: Thin solid films.

Volume: **220**
Issue:
Month/Year: **1992**

Pages: **284 288**

Article Author:
Article Title: 35. F. Yuan, Y. Shi, L.V. Knight, R.T. Perkins and D.D. Allred; USING THIN-FILM STRESS TO PRODUCE PRECISION, FIGURED X-RAY OPTICS

RUSH - GWLA

Borrower: UBY

Brigham Young University
3421 Lee Library *** ILL
One Lee Lane
Provo, Ut 84602
Fax:
Ariel:

Patron: Allred, David

ILL Number: **15343251**

Wash U ILL Office Hours:
Monday - Friday, 8:30am - 5pm
Phone: 314-935-7193
ill@wulib.wustl.edu

Thin Solid Films, 220 (1992) 284–

Using thin film stress to produce precision, figured X-ray optics

F. Yuan, Y. Shi, L. V. Knight, R. T. Perkins and D. D. Allred

Center for X-Ray Imaging and Department of Physics and Astronomy, Brigham Young University, Provo, UT 84602 (USA)

Abstract

We are studying the possibility of producing precision, aspherical mirrors for X-rays and visible light. Our study examines the use of ultrastructure processing to replace mechanical methods of material removal. The method starts with a chemically–mechanically polished, flat silicon wafer. The aim is to preserve atomic scale smoothness of the surface wafer while the wafer is bent to a desired figure. We report measurements of the mechanical properties of various stressing layers. This involves measuring the deformation of several thin silicon wafers coated with chemically vapor deposited nickel and boron films of known thickness. We have found that, under normal conditions, the film does not add to the microroughness of the substrate on either the front or the back surfaces. Film and substrate thicknesses, however, vary by as much as 10%. This is the present limit on figure accuracy. We have developed a model that describes bending of B/Si and Ni/Si structures. The model relates stress and Young's modulus to the measured thickness of the film, and the thickness and curvature of the substrate. This approach is used to measure the stress and Young's modulus for boron and nickel films. The Young's modulus E_f was 3.05×10^{12} Pa for the boron films and 1.4×10^{10} Pa for the nickel films. From the relationship developed and verified for predicting the radii of curvature of the substrate, it may be possible to define a film thickness pattern which would provide a desired optical figure.

1. Introduction

We are investigating the production of precision, aspherical mirrors for X-rays and visible light. Our study focuses on the question, can ultrastructure processing be used to replace mechanical methods of material removal to produce figured optics? We begin with a chemically–mechanically polished, flat silicon wafer. The aim is to preserve the initial smoothness of the surface wafer, which we have found by scanning probe microscopy is typically about 1 nm r.m.s., while the wafer is controllably bent to the desired figure. The wafer is bent by the build-up of stress of predetermined amounts and at predetermined locations. This is done through the formation of stressed films or might be done through selective ion implantation. The thin films examined include silicon dioxide, silicon nitride, metals and boron. Borophosphosilicate glasses have been considered. The bending can also be modulated to produce complex shapes by controlled thinning of the wafer, prior to deposition, of selected regions of the back surface of the wafer. The stressed layers together with the thinned pattern precisely determine the final topology of the smooth surface. This method is potentially capable of producing an optical element of an arbitrarily precise figure which is also atomically smooth.

In this paper we report, first, on the development of a two-dimensional model which is useful in studying thin film stress on thin silicon wafers and, second, on the use of the model to obtain the modulus and stress of films from experimental measurements. These are key activities in obtaining precision bending. The model is based on a closed form solution to the bending problem. The model assumes that the film stress is independent of film thickness and that the effect of boundaries can be ignored.

The experimental measurements also allow us to examine the feasibility of producing figured optical surfaces with respect to two key questions: is surface smoothness maintained for bended wafers and to what precision can optical figure be obtained?

The roughness of the mirror surface must be small compared with the wavelength used. The surface roughness as measured with a WYKO profilometer was found to be typically in the range 1.2–1.6 nm r.m.s. both before and after bending and on both the coated and uncoated surfaces. As long as the surface roughness of the film is close to the roughness of the substrate, the film surface is considered smooth.

With respect to the figure the key issue has proven to be uniformity. The substrate and stressing films must have a uniform film thickness and small structural defects so that the film/substrate structure has a homogeneous mechanical behavior. The results indicate that the model accurately describes the figure, near their center, of wafers that are stressed by thin film deposition. However, the accuracy of the actual figure is limited by deposition uniformity and any inhomo-

geneities of the substrate. The thin film thickness will vary from point to point by as much as 10%. This is the present limit on the figure accuracy.

2. Model

The model establishes a relationship among the elastic constants and thickness of silicon wafers, the stress, thickness and Young's modulus of the thin film, and the radius of curvature of the bent structure. Substrates in our experiments were (110) silicon wafers since these can be anisotropically etched into ribbed structures. The theory is based on Hooke's law applied to the elastic properties of silicon wafers. It predicts the behavior of the wafer in terms of the silicon elastic constants. Since there are only small strains during the process of curving the structure, the application of Hooke's law is reasonable. For simplicity, the crystallographic axes x, y, z, which indicate [100], [010], and [001] respectively, are now changed into x', y', z' (Figs. 1(b) and 1(c)). Thus, the stress–strain relation is

$$\epsilon'_{ij} = s'_{ijkl}\sigma'_{kl}, \quad i, j, k, l = 1, 2, 3 \tag{1}$$

where ϵ'_{ij} and σ'_{kl} are components of the strain and stress tensor respectively, and s'_{ijkl} are the tensor components of the elastic compliance constant. By considering symmetry relationships [1] we can identify six independent stress tensor elements σ' and six strain tensor elements ϵ'. There are 36 compliance tensor elements s'. The relationship can be further simplified because chemically vapor deposited boron and nickel films, the films used in this study, respectively, are amorphous [2] and polycrystalline [3] and act quasi-isotropically on the substrate. Thus, the elements of the stress tensor that respresent shear stress are zero. In addition, the stress relationship in the x' direction is approximately zero because the film is thin in this direction (see Fig. 1(c)). The stress tensor becomes

$$\boldsymbol{\sigma}' = (0, \sigma'_2, \sigma'_3, 0, 0, 0) \tag{2}$$

Thus, the stress–strain equation can be rewritten as

$$\epsilon'_i = s'_{ij}\sigma'_j, \quad i = 1, 2, \ldots, 6; \quad j = 2, 3 \tag{3}$$

which contains three axial strain components ($i = 1, 2, 3$) and three shear strain components ($i = 4, 5, 6$). The elastic compliance tensor elements s'_{ij} can be expressed in terms of the elastic compliance

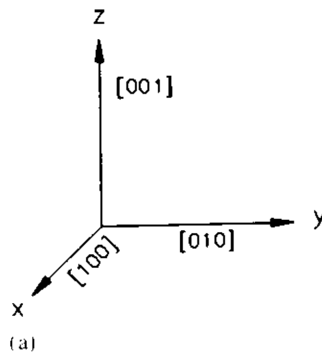

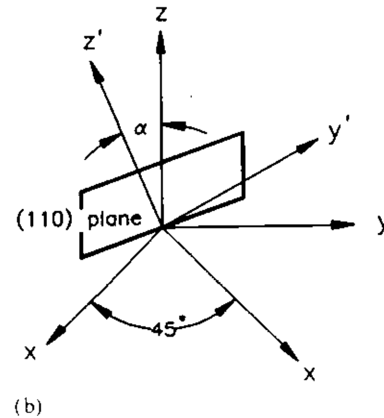

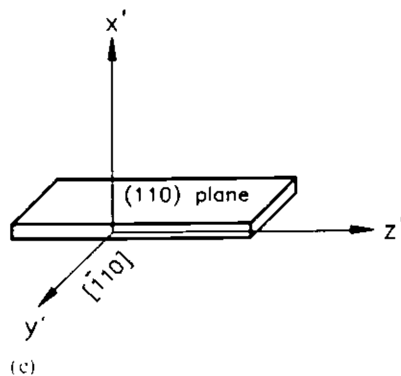

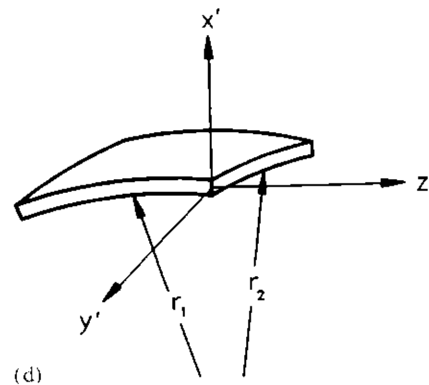

Fig. 1. Crystal lattice coordinate system.

constants in the silicon crystallographic axes and the direction cosines of a coordinate transformation [4].

The stresses in the (110) plane are taken to be isotropic, *i.e.* $\sigma'_2 = \sigma'_3$. Then

$$\epsilon'_3 = (s'_{32} + s'_{33})\sigma'_3 = s'_{\text{equiv}}\sigma'_3 \tag{4}$$

The maximum and the minimum values of s'_{equiv} occur at α (see Fig. 1(b)) and equal 0° and 90° respectively [3]. According to the mechanics of materials [5], $\epsilon'_4 = \epsilon'_5 = \epsilon'_6 = 0$. Then

$$\epsilon'_i = s'_{ij}\sigma'_j, \quad i = 1, 2, 3, \quad j = 2, 3 \tag{5}$$

The curvature occurs in the y'–z' plane. Thus, ϵ'_2 and ϵ'_3 are the relevant strain elements. These give the stress–strain relations for bending of a thin film/substrate combination such as a B/Si or an Ni/Si structure:

$$\epsilon'_3 = s'_{32}\sigma'_2 + s'_{33}\sigma'_3$$

$$\epsilon'_2 = s'_{22}\sigma'_2 + s'_{23}\sigma'_3 \tag{6}$$

Now we can obtain an expression that predicts the bending of film/silicon structures. A thin film under stress will bend its substrate to relax the stress. The intrinsic stress is the stress before relaxation. The final stress is the equilibrium stress. The intrinsic film stress σ_{in} is assumed to be independent of boron and nickel film thicknesses. This is because the stress at the film–silicon interface is not lattice mismatch related since boron and nickel films are amorphous and polycrystalline respectively, and the interdiffusion at the interface is negligible even at deposition temperature [2]. Thus, thermal mismatch between the film–silicon boundary is the main contributor to the film stress. Hence [6], the film stress is expected to be independent of thickness.

Now, consider the bending process. From a conceptual, step-by-step, point of view, it is imagined that, as a first step, the film is deposited on a flat silicon substrate. After the deposition, it is imagined that, by some means, the substrate has been kept flat and stress free, so that the film is under maximum tensile stress σ_{in} (see Fig. 2(c)). In the third conceptual step the tensile stress in the film relaxes somewhat while the stress in the substrate builds up (see Fig. 2(d)). This continues until the sum of forces across the cross-section is zero. Then bending is allowed to occur to counterbalance the moments induced by contraction (see Fig. 2(e)). The process ends when the sum of moments across the cross-section is zero.

Let E_{f} and E_{s} be the Young's moduli of the film and the substrate respectively, along the direction where the most curvature occurs. Also, t_{f} and t_{s} are the thickness of the film and the substrate. During contraction (see Fig. 2(d)), film tension relaxes and substrate compression increases until the forces are equal at equilibrium. Let the strain due to contraction be δ at that point. At equilibrium, tension in the film is given by $\sigma' = \sigma_{\text{in}} - E_{\text{f}}\delta$ and compression in the substrate is given by $\sigma'' = E_{\text{s}}\delta$. The condition of zero net force requires that $\sigma'' t_{\text{s}} = \sigma' t_{\text{f}}$. Thus

$$\delta = \frac{\sigma_{\text{in}} t_{\text{f}}}{E_{\text{s}} t_{\text{s}} + E_{\text{f}} t_{\text{f}}}$$

The tensile force in the film and the compressive force in the substrate form a moment per unit width in the flat structure:

$$M_1 = \sigma'' t_{\text{s}} \frac{t_{\text{s}} + t_{\text{f}}}{2} = \frac{\sigma_{\text{in}} t_{\text{f}} t_{\text{s}} E_{\text{s}}(t_{\text{s}} + t_{\text{f}})}{2(E_{\text{s}} t_{\text{s}} + E_{\text{f}} t_{\text{f}})} \tag{7}$$

These opposing forces drive the bending. The condition of equilibrium, zero total moment over any cross-section, puts constraints on the stress. Consider Fig. 2(b). To achieve equilibrium, the structure bends. The strain associated with the bending is shown in Fig. 2(e) and the corresponding stress in Fig. 2(f). In Fig. 2(e), d represents the position of the surface with neutral strain. There are two constraints that uniquely determine the bending. The first is that the net force in Fig. 2(f) is zero. The second is that the moment in Fig. 2(f) equals that in Fig. 2(d) in magnitude and is opposite in direction.

Using these two conditions and the assumption that t_{s} is much greater than t_{f}, we obtain

$$6r\sigma_{\text{in}} t_{\text{f}} t_{\text{s}}(t_{\text{s}} + t_{\text{f}}) = E_{\text{f}}(t_{\text{s}} + t_{\text{f}})^4 + (E_{\text{s}} - E_{\text{f}}) \times [t_{\text{s}}^4 - (E_{\text{f}}/E_{\text{s}})t_{\text{f}}^4] \tag{8}$$

If the elastic parameters E_{s} and E_{f} and the intrinsic film stress σ_{in} are known, film thickness t_{f} and substrate thickness t_{s} will determine the radius of curvature of the bending. For $R = r_1/r_{\text{s}}$, r_1 is the large radius and r_{s} is the small radius; we can find E_{s} using the equation

$$\frac{1}{E_{\text{s}}} = s'_{33} + s'_{32}\frac{s'_{33} - Rs'_{32}}{Rs'_{22} - s'_{32}} \tag{9}$$

E_{f} can be found through experimental measurements of t_{f}, t_{s}, and r for different thickness samples of the same film/substrate pair. The values of the components s'_{ij} can be found in Wortman's paper [4]. At least two samples are required to solve the two simultaneous equations for two unknowns, E_{f} and σ_{in}. Thus, E_{f} and σ_{in} are obtained.

3. Experimental results

The silicon wafers in this experiment were 5.1 mm in diameter, 76 μm ± 7.6 μm thick, polished on both sides. The substrates were coated on one side with a boron or a nickel film by chemical vapor deposition (CVD), hot

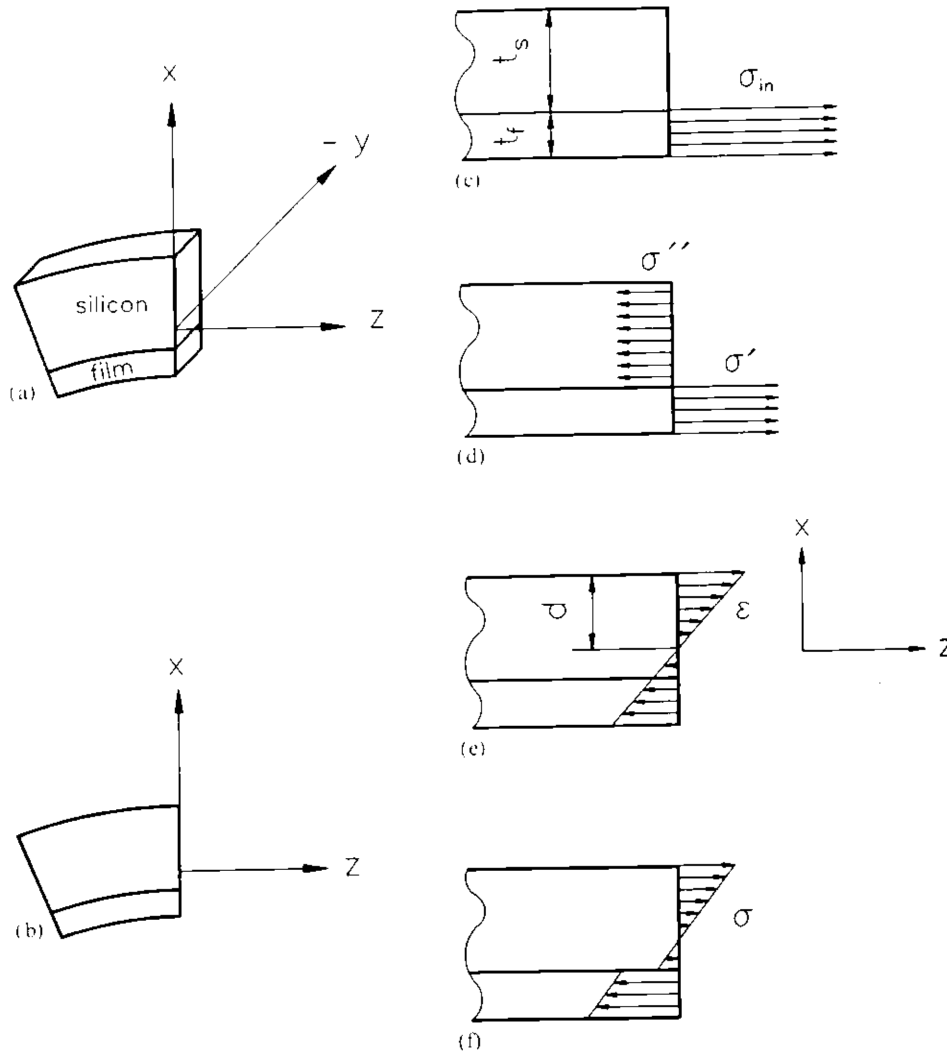

Fig. 2. (a) Bent film/silicon structure, with the largest strain in the z direction and the smallest strain in the y direction. (b) Representing the bent structure with the axes x and y. (c) Film/silicon structure before the silicon wafer deformation occurs. (d) Structure contracts while remaining flat. (e) Strain associated with structure bending. (f) Stress associated with structure bending.

wall CVD for boron and cold wall CVD for nickel. Boron is deposited by using diborane at a nominal temperature of 450 °C. The source of the nickel film is the pyrolysis at 320 °C of $Ni(CO)_4$ in a CO gas stream. Several film/silicon structures were fabricated with various different film thicknesses.

E_s is evaluated by using eqn. (9). With the fact that for these structures $R = r_l/r_s > 20$, eqn. (9) is approximated as

$$\frac{1}{E_s} = s'_{33} - \frac{s'^2_{32}}{s'_{22}} \tag{10}$$

Thus,

$E_s = 1.448 \times 10^{11}$ Pa

E_f is determined by a least-squares fit of experimental data to a parametric equation derived from eqn. (8).

The results for boron films are

$E_f = 3.05 \times 10^{12}$ Pa

$\sigma_{in} = 9.03 \times 10^8$ Pa

and for nickel films are

$E_f = 1.4 \times 10^{10}$ Pa

$\sigma_{in} = 6.4 \times 10^8$ Pa

The resultant film/silicon structures were then optically characterized with respect to figure, surface waviness, and surface roughness which will be considered sequentially.

3.1. Figure

The figure of the curved film/silicon structures was obtained by measuring r_s and r_l with a WYKO profi-

lometer. The measurements were made at points along imaginary lines parallel to the [$\bar{1}$10] axis.

The center of the sample surface is cylindrical over a range of at least 3 cm. Deviation from a cylindrical surface is caused by surface waviness. There is at most 10% relative difference in radius of curvature between sample edges and sample center. We believe this is caused by the effect of the wafer boundary. Finite wafer size effects are not considered in the theory.

3.2. Surface waviness

These are surface undulations measured on a millimeter to centimeter scale. The r_s values show a distinct irregularity, surface waviness, going from one end of the sample to the other. This is confirmed by a Ronchi ruling test [7, 8]. The test was also used to measure the variation in r_s to be approximately 5.7%. We considered two possibilities for the cause of surface waviness.

(1) The surface waviness in the flat silicon wafer used as a substrate is carried onto the curved structures.

(2) The thickness non-uniformity in the stressing film and the substrate is also carried onto the curved structures.

A Twyman–Green interferometer was built to test the surface flatness of flat (110) 76 μm thick silicon wafers. An optical flat of $\lambda/4$ quality was used in the interferometer as a flat standard. A surface waviness of up to 8% with respect to the nominal wafer thickness was found from the fresh silicon wafers used in this study. The film thickness non-uniformity was up to 7% with respect to the average film thickness [3]. It appears that both effects caused waviness in curved film/silicon structures.

3.3. Surface roughness

These are surface undulations in an area on the 10–100 μm scale. Roughness measurements were taken with a WYKO profilometer. The focus of surface roughness evaluation is on whether the structure bending introduces roughness to the surface. The roughness of the mirror surface must be small compared with the wavelength used. The stressing films must have a uniform film thickness and small structural defects so that the film/substrate structure has a homogeneous mechanical behavior. This requirement also determines the side of the silicon wafer on which the stressing film should be placed. The silicon wafers are polished on both sides. The surface roughness as measured with a WYKO profilometer was in the range 1.2–1.6 nm r.m.s. Based on measurements of all the samples prepared there is no correlation between the surface roughness and the amount of structure bending. The films do not introduce roughness.

4. Conclusions

Our model accurately predicts the figure over the center portion of substrates that are stressed by thin film deposition. The key issues are the uniformity of the deposited film and substrate quality. Using optimum deposition parameters, the thin film does not add to the microroughness of the substrate. However, non-uniform deposition and substrate variation can cause waviness in the figure. The model can be used to design a specific aspherical figure. However, the accuracy of the actual figure is limited by deposition non-uniformity and substrate error. This means that thin film thickness will vary from point to point by about 10%. This is the present limit on the figure accuracy. It may be possible to produce more uniform films by using atomic layer epitaxy, but of equal importance is the fact that the substrates are not uniform. A real time–*in situ* correction process is required which will measure the figure of a bent substrate and correct it *in situ*. The solution to these problems seems straightforward: interaction between the model and the fabrication. However, work and innovation will be required to make it practical.

References

1 J. F. Nye, *Physical Properties of Crystals*, Clarendon, Oxford, 1975, p. 131.
2 F. Yuan, Characterization of boron films prepared by chemical vapor deposition and their applications in X-ray imaging, *Ph.D Dissertation*, Brigham Young University, 1991, pp. 10–31.
3 Y. Shi, Development and modeling of cylindrically shaped multilayer X-ray reflectors, *Ph.D. Dissertation*, Brigham Young University, 1991, p. 55.
4 J. J. Wortman and R. A. Evans, *J. Appl. Phys.*, *36* (1965) 153
5 R. D. Cook and W. C. Young, *Advanced Mechanics of Materials*, Macmillan, Basingstoke, 1985.
6 J. A. Thornton and D. W. Hoffman, *Thin Solid Films*, *171* (1989) 5.
7 A. Kirkham, in A. G. Ingalls (ed.), *Amateur Telescope Making*, Vol. 1, Freeman, New York, 1953.
8 A. Cornejo-Rodriguez, in D. Malacara (ed.), *Optical Shop Testing*, Wiley, New York, 1978.